

Rotary Heat Exchangers With Time Varying or Nonuniform Inlet Temperatures

M. J. Brandemuehl

Research Division,
Carrier Corporation,
Syracuse, N.Y. 13221

P. J. Banks

Division of Energy Technology,
Commonwealth Scientific and
Industrial Research Organization,
Hightett, Victoria 3190
Australia

The performance of a counterflow, rotary heat exchanger operating with either transient or nonuniform inlet temperatures is investigated. The effect of transient inlet temperatures is analyzed in terms of the response of the outlet fluid temperatures to a step change in temperature of one of the inlet fluid streams. The effect of temperature nonuniformities is analyzed in terms of the change in steady-state effectiveness due to a circumferential temperature distribution in one of the inlet fluid streams. These temporal and spatial variations are explored using three different methods of analysis. An equilibrium analysis, assuming infinite heat transfer coefficients, is developed from kinematic wave theory. It is used to qualitatively describe the heat transfer process and define the upper limit of performance. A finite difference model of the governing differential equations, using finite transfer coefficients, is employed to obtain a detailed numerical analysis of heat exchanger performance. Results for the complete range of matrix to fluid capacity rate ratio are presented for a balanced and symmetric regenerator. At moderate capacity rate ratios, the numerical analysis predicts unusual temporal periodicity in the transient response. An experimental analysis has also been conducted using a counterflow, parallel passage, rotary heat exchanger made from polyester film. The results are used to substantiate predictions of the numerical model.

Introduction

A rotary heat exchanger, or regenerator, is a regenerative heat exchange device in which a rotating porous matrix of material is alternately exposed to hot and cold fluid streams. A schematic diagram of such a regenerator is shown in Fig. 1, with the fluid streams flowing in countercurrent directions. The counterflow configuration is more common and gives higher performance than the alternative unidirectional flow configuration. Traditionally, these regenerators have been employed in gas turbine engines. Recently, they have assumed importance in solar air-conditioning systems and other air-to-air heat recovery processes requiring a compact high-performance unit.

This paper investigates the performance of a counterflow, rotary regenerator operating with either transient or nonuniform fluid inlet temperatures. A temporal step change and a circumferential nonuniformity are considered. Three different methods of analysis are employed: an equilibrium analysis, a numerical analysis, and an experimental analysis. The equilibrium analysis is used to define the upper limit of performance, while the numerical analysis provides detailed results of use to the designer. The experimental analysis verifies these theoretical models.

While this paper specifically examines rotary regenerator performance, a regenerative heat exchanger may also be of fixed-matrix form in which the hot and cold fluid streams are alternately passed through two or more fixed porous matrices. The performance of a rotary regenerator is based on the circumferential-averaged fluid outlet temperature, while that of a fixed-matrix regenerator is based on the time-averaged fluid outlet temperature during each period. The theoretical analysis is the same for both types of regenerator under steady periodic conditions with uniform inlet temperatures. However, the analysis of the two types of regenerators differs when considering transient or nonuniform inlet temperatures.

In the case of nonuniform inlet temperature, circumferential nonuniformity in inlet fluid temperature to a rotary regenerator corresponds to time variation in inlet fluid temperature during each period in a fixed-matrix regenerator. In the case of transient inlet temperature, the response is presented in terms of the temporal variation of the circumferential-averaged fluid outlet temperature for the rotary regenerator and in terms of the temporal variation of the time-averaged fluid outlet temperature in each successive period for the fixed-matrix regenerator. While the transient response of a rotary regenerator is continuous with time, the response of a fixed matrix regenerator is comprised of a series of discrete points, separated in time by the period duration. While the overall responses of the two types of regenerators are the same, the response of the fixed-matrix regenerator is unable to resolve transient effects on a time scale less than the period duration.

The performance of a regenerator operating under steady periodic conditions with uniform inlet temperatures has been investigated by many authors, and the results are available in the literature [1-4]. However, there have been few theoretical or experimental investigations of rotary regenerators operating with transient inlet temperatures, and none for

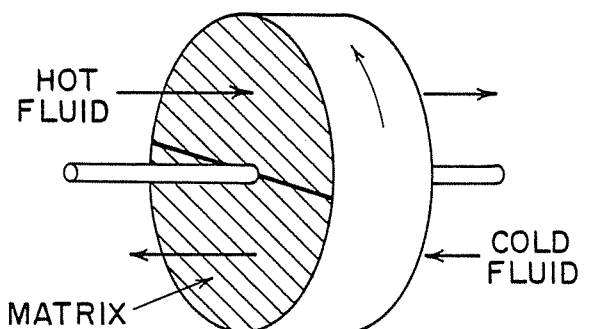


Fig. 1 Schematic diagram of a counterflow rotary heat exchanger

Contributed by the Heat Transfer Division and presented at the ASME Winter Annual Meeting, Washington, D.C., November 15-20, 1981. Manuscript received by the Heat Transfer Division September 11, 1981.

nonuniform inlet temperatures to the authors' knowledge. London et al. [5] have examined the transient response of a gas turbine regenerator to a step change in one fluid inlet temperature, using limited computer solutions and an analogy with recuperative heat exchanger theory. Their analysis considered balanced and symmetric regenerators operating at matrix to fluid capacity rate ratios much larger than unity. Chao [6] presents a brief discussion of transients in rotary regenerators using limited theoretical and experimental results.

Willmott and Burns [7, 8] used numerical analysis to predict the transient response of unbalanced and asymmetric fixed-matrix regenerators, considering matrix to fluid capacity rate ratios larger than unity. Shah [9] provides a discussion of transients in recuperative and regenerative heat exchangers, including results from [5, 7, 8].

While the literature generally contains transient results for large matrix to fluid capacity rate ratios, this paper includes results for regenerators operating at small capacity rate ratios. A well-designed regenerator for sensible heat transfer will always be operating at large capacity rate ratios to maximize regenerator efficiency. However, regenerators for heat and mass transfer, such as rotary dehumidifiers or energy recovery units, can be analyzed using an analogy with heat transfer which employs sensible heat regenerator theory [10-12]. This analogy method often requires sensible heat regenerator results for small capacity rate ratios. Recognizing this application, results for the complete range of matrix to fluid capacity rate ratios have been included.

Theoretical Investigation

Governing Equations. The basic equations governing the transfer of heat in regenerators and the measures of performance are defined in this section. Several assumptions have been made in the derivation of these equations. It is assumed that heat transfer between the fluid and matrix is by convection only. As such, heat conduction in the axial and circumferential directions, in both the fluids and matrix, is assumed to be negligible. It is assumed that the temperatures of both the fluids and matrix are uniform in the radial direction. The specific heats of the fluids and matrix are considered constant, as are the heat transfer coefficients between the fluids and matrix. Leakage between the two

fluid streams is assumed to be negligible, and the capacity of the matrix in each period is assumed to be much larger than the capacity of the fluid contained in its porous structure.

An energy balance on an element of the matrix yields the following differential equations [10]

$$v_i \frac{\partial t'}{\partial x'} + \mu_i \sigma_i \frac{\partial T'}{\partial \theta'} = 0 \quad (1)$$

$i = 1, 2$

$$\mu_i \sigma_i \frac{\partial T'}{\partial \theta'} + J_i (T' - t') = 0 \quad (2)$$

The subscript i refers to periods 1 or 2. The x' -direction in each period is the direction of fluid flow. Equations (1) and (2) can be rewritten using dimensionless parameters and variables to give the following

$$\frac{\partial t}{\partial x} + \beta_i C_i^* \frac{\partial T}{\partial \theta} = 0 \quad (3)$$

$i = 1, 2$

$$\beta_i C_i^* \frac{\partial T}{\partial \theta} + Ntu_i (T - t) = 0 \quad (4)$$

Equations (3) and (4) are constrained by the boundary and initial conditions: $t = t_{i,in}$ at $x = 0$ and $T(x)$ is known at $\theta = 0$. In periodic steady-state operation, the axial matrix temperature distribution at time θ is equal to that at $\theta + n$, where n is any integer. In these equations, the dimensionless fluid and matrix temperatures are defined as

$$t = \frac{t' - \overline{t'}_{2,in}}{\overline{t'}_{1,in} - \overline{t'}_{2,in}} \quad (5)$$

$$T = \frac{T' - \overline{t'}_{2,in}}{\overline{t'}_{1,in} - \overline{t'}_{2,in}}$$

where

$$\overline{t'}_{1,in} = \frac{1}{\beta_1} \int_0^{\beta_1} t'_{1,in} d\phi$$

$$\overline{t'}_{2,in} = \frac{1}{\beta_2} \int_{\beta_1}^1 t'_{2,in} d\phi \quad (6)$$

Nomenclature

A_v = heat transfer area per unit volume, m^2/m^3	perature, defined in equation (5)	η_i = regenerator efficiency defined by equation (7)
c_p = specific heat of fluid, $J/kg^\circ C$	t' = fluid temperature, $^\circ C$	θ = dimensionless time variable, defined as $\theta'/(P_1 + P_2)$
C_i^* = matrix to fluid capacity rate ratio of period i , defined as $(\mu\sigma L/Pv)_i$	T = dimensionless matrix temperature, defined in equation (5)	θ' = time variable, s
e_i = the transient response of period i , defined by equation (10)	T' = matrix temperature, $^\circ C$	μ_i = ratio of mass of matrix to mass of contained fluid in period i
h = convective heat transfer coefficient, $W/m^2^\circ C$	v_i = velocity of fluid in matrix passages, m/s	ρ = density of fluid, kg/m^3
J_i = matrix-fluid convective transfer coefficient per unit capacity of fluid in period i , defined as $J_i = hA_v/\rho c_p \epsilon$, $1/s$	x = dimensionless length variable, defined as x'/L	σ_i = ratio of specific heat of matrix to specific heat of fluid in period i
L = length of matrix, m	x' = length variable, m	ϕ = dimensionless azimuthal angle, defined as $\phi'/2\pi$
n = an integer defined in Table 2	β_i = dimensionless duration of period i , defined as $P_i/(P_1 + P_2)$	ϕ' = azimuthal angle, rad
Ntu_i = number of transfer units in period i , defined as $(JL/v)_i$	β_s = dimensionless azimuthal position of change in nonuniform temperature distribution of Fig. 4	Subscripts
P_i = duration of period i , s	δ = half the magnitude of temperature change in Fig. 4	i = period i , $i = 1, 2$
t = dimensionless fluid tem-	ϵ = porosity of matrix	in = at regenerator inlet
		out = at regenerator outlet
		Superscripts
		= spatial average

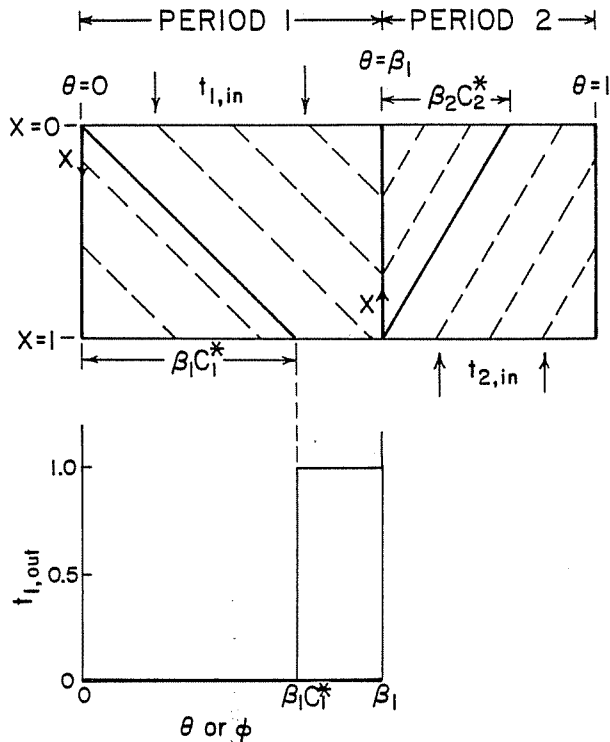


Fig. 2 Wave diagram for regenerator under steady periodic operation with $C_1^* < 1$ and $C_2^* < 1$. Period 1 outlet temperature distribution for constant inlet fluid temperature. The coordinate x increases in the flow direction in each period.

The use of Ntu_i and C_i^* as regenerator parameters is based on the nomenclature of Kays and London [3]. (In the nomenclature of Hausen [1], $Ntu_i = \Lambda_i$ and $C_i^* = \Lambda_i/\Pi_i$.) While Kays and London refer to the fluid streams as having either the minimum or maximum capacity rate, such a designation is inappropriate for this paper. Instead, for the analyses of this paper, the fluid stream with variable inlet conditions, in the form of spatial nonuniformities or time variations, will be referred to as period 1. Period 2 refers to the fluid stream with constant inlet temperature.

The performance of the regenerator will be characterized by two separate indicators. Under steady-state conditions, it is characterized by the regenerator efficiency, η_i

$$\eta_i = \frac{\bar{t}_{i,out} - \bar{t}_{i,in}}{\bar{t}_{j,in} - \bar{t}_{i,in}} \quad i=1,2 \quad (7) \quad j=3-i$$

By definition of the dimensionless inlet temperatures in equations (5), $\bar{t}_{1,in} = 1$ and $\bar{t}_{2,in} = 0$, and equation (7) yields the following

$$\eta_1 = 1 - \bar{t}_{1,out} \quad (8a)$$

$$\eta_2 = \bar{t}_{2,out} \quad (8b)$$

For a regenerator operating under steady periodic conditions, conservation of energy requires that the following condition is satisfied.

$$C_2^* \eta_1 = C_1^* \eta_2 \quad (9)$$

For a balanced regenerator, $C_1^* = C_2^*$, $\eta_1 = \eta_2$, and the regenerator efficiency is equal to the regenerator effectiveness of Kays and London [3].

The response of a regenerator to a step change in inlet fluid temperature will be characterized by the transient response, e_i .

$$e_i = \frac{\bar{t}_{i,out}(\theta) - \bar{t}_{i,out}(\theta=0)}{\bar{t}_{i,out}(\theta=\infty) - \bar{t}_{i,out}(\theta=0)} \quad i=1,2 \quad (10)$$

The temperatures used in equation (10) are the circumferential-average temperatures at the outlet of period i .

Physically, the solution of equations (3) and (4) describes the behavior of a wedge-shaped segment of the matrix, and its associated fluid, as it rotates through the two fluid streams with time. The regenerator efficiency and transient response, however, are defined in terms of spatial average temperatures, averaged over the azimuthal angle, at a particular time.

For regenerators operating under periodic steady-state conditions, the time average outlet temperature of any segment is equal to the spatial average outlet temperature at any time. In effect, the variable θ of equations (3) and (4) can simply be replaced by the azimuthal angle variable, ϕ . However, for regenerators operating under transient inlet conditions, the spatial distribution at a particular time must be obtained by solving equations (3) and (4) for segments of the matrix originally at every angular position.

Equilibrium Analysis. The equilibrium analysis assumes infinite heat transfer coefficients between the matrix and the fluid ($Ntu_i = \infty$). As such, the analysis defines the upper limit of regenerator performance. The assumption also allows the regenerator to be analyzed using kinematic wave theory, a simple yet powerful analytical tool which provides a graphical method for describing the dynamics of the heat transfer process.

Under the conditions $Ntu_i = \infty$, the matrix and fluid are in thermal equilibrium at every location ($t = T$) and equation (3) can be rewritten as equation (11).

$$\frac{\partial T}{\partial x} + \beta_i C_i^* \frac{\partial T}{\partial \theta} = 0 \quad (11)$$

Equation (11) is of the form of a kinematic wave equation [13, 14]. The solution is such that T is a constant in the (x, θ) -plane in the directions $d\theta/dx = \beta_i C_i^*$. Therefore, T will be constant along lines of constant $\theta - \beta_i C_i^* x$, and since both β_i and C_i^* are constants, these lines will be straight and parallel.

To illustrate this point, consider a regenerator, described by equation (11), operating under steady periodic condition, with $C_1^* < 1$ and $C_2^* < 1$. Figure 2 shows a wave diagram for this situation, which traces the temperature distribution of a segment of the matrix from the time it enters period 1 ($\theta=0$) until it exits from period 2 ($\theta=1$). The dashed lines correspond to lines of constant T , and the solid lines correspond to the position of the wavefront between period 1 and period 2 temperatures.

A particular feature of kinematic wave equations of the form of equation (11) is that the temperature at any (x, θ) can be determined from either the initial or boundary conditions. Thus, referring to Fig. 2, the temperature distribution at the outlet of period 1 from $\theta=0$ to $\theta=\beta_1 C_1^*$ corresponds to the temperature distribution in the matrix at the beginning of the period ($\theta=0$), which in turn corresponds to the period 2 inlet fluid temperature distribution at its inlet from $\theta=1 - \beta_2 C_2^*$ to $\theta=1$. Similarly, the outlet temperature between $\theta = \beta_1 C_1^*$ and $\theta = \beta_1$ is equal to the inlet temperature between $\theta = 0$ and $\theta = 1 - \beta_1 C_1^*$. Figure 2 also shows the period 1 outlet temperature distribution when both the inlet fluid streams have uniform inlet temperatures.

Since the regenerator is operating under steady periodic conditions, Fig. 2 also represents the spatial temperature distribution within the matrix when θ is replaced by ϕ . The regenerator efficiency can then be obtained directly from Fig. 2. Thus, for uniform inlet fluid temperatures, $t_{1,in} = 1$ and $t_{2,in} = 0$, the outlet temperature is 0 from $\phi = 0$ to $\phi = \beta_1 C_1^*$ and 1 from $\phi = \beta_1 C_1^*$ to $\phi = \beta_1$. Hence equations (7) give $\eta_1 = C_1^*$ and $\eta_2 = C_2^*$. For nonuniform inlet fluid temperatures, with $t_{1,in} = f_1(\phi) = f_1(\theta)$ and $t_{2,in} = f_2(\phi) = f_2(\theta)$, the outlet temperatures must be integrated to obtain the regenerator efficiencies. The results given in Table 1 for regenerator ef-

efficiency η_1 can be derived from equations (8) for the cited ranges of C_1^* and C_2^* .

The kinematic wave concept can also be used in the analysis of regenerators operating under transient inlet conditions due to a step change in inlet fluid temperature. At times $\theta < 0$, the matrix is operating under steady periodic conditions at the initial fluid inlet states. At $\theta = 0$, a step change is applied to the period 1 inlet fluid temperature while the period 2 inlet fluid temperature remains unchanged. Because of the linearity of equations (3), (4), and (11), and the definition of the transient response, e_i , the results are independent of the particular choice of initial and final inlet fluid temperatures. Recognizing this fact, the initial inlet temperatures are both set to zero and the period 1 final inlet fluid temperature is set equal to unity. Notice that e_1 is the outlet fluid temperature response of the period in which the step change occurred while e_2 is the response of the opposite period.

In the analysis of regenerators operating under periodic steady state conditions, the solution to equation (11) was applied only to the segment of the matrix which, at $\theta = 0$, was in the position $\phi = 0$. However, for a regenerator operating under transient inlet conditions, the spatial temperature distribution can only be obtained by applying the solution of equation (11) to all segments of the matrix.

To illustrate this technique, consider a balanced symmetric

regenerator ($C_1^* = C_2^*$, $\beta_1 = \beta_2 = 0.5$) with $C_1^* = 0.8$. At $\theta = 0$, $t_{1,in} = t_{2,in} = 0$ and the matrix is uniformly at $T = 0$. The period 1 inlet fluid temperature is then changed to $t_{1,in} = 1$. Figure 3 shows the spatial temperature distribution within the matrix at four values of time, $\theta = 0.2, 0.4, 0.6, 0.8$. At $\theta = 0.2$, the temperature change wavefront has begun to propagate through the matrix. The fluid outlet temperature of period 1 remains unchanged with $e_1 = 0$. However, the fluid outlet state of period 2 has already been changed to $e_2 = 0.25$. At $\theta = 0.4$, the temperature wavefront in period 1 has emerged from the matrix causing a step increase in the period 1 response from $e_1 = 0$ to $e_1 = 1$. The fluid outlet temperature of period 2 has continued to increase giving $e_2 = 0.5$. As the temperature wavefront has propagated through the matrix in period 1, the axial temperature distribution of the matrix entering period 2 has continually changed. Since the wavefront has propagated through the matrix in period 1 at $\theta = 0.4$, the axial distribution of the matrix entering period 2 will henceforth remain constant at $T = 1$. At $\theta = 0.6$, the period

Table 1 Period 1 regenerator efficiency for nonuniform inlet temperature from equilibrium analysis. Period 2 efficiency defined as $\eta_2 = (C_2^*/C_1^*)\eta_1$.

$C_1^* \leq 1$	$\eta_1 = 1 - \frac{1}{\beta_1} \int_0^{\beta_1(1-C_1^*)} f_1(\phi) d\phi - \frac{C_1^*}{\beta_2 C_2^*} \int_{1-\beta_2 C_2^*}^1 f_2(\phi) d\phi$
$C_2^* \leq 1$	
$C_1^* \geq 1$	$\eta_1 = 1 - \frac{C_1^*}{\beta_2 C_2^*} \int_{1-(\beta_2 C_2^*/C_1^*)}^1 f_2(\phi) d\phi$
$C_2^* \leq C_1^*$	
$C_2^* \geq 1$	$\eta_1 = 1 - \frac{1}{\beta_1} \int_0^{\beta_1(1-(C_1^*/C_2^*))} f_1(\phi) d\phi$
$C_1^* \leq C_2^*$	

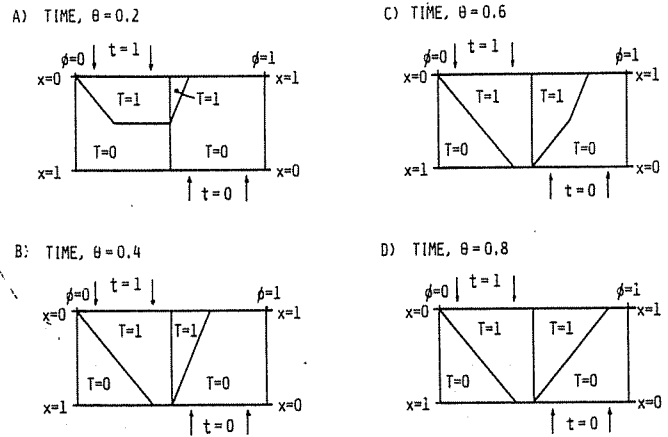


Fig. 3 Spatial temperature distributions for equilibrium analysis of transient response at $\theta = 0.2, 0.4, 0.6, 0.8$ with $C_1^* = C_2^* = 0.8$ and $\beta_1 = \beta_2 = 0.5$. The coordinate x increases in the flow direction in each period.

Table 2 Regenerator transient response for equilibrium analysis

C_1^*	θ range	Response, e_i
$C_1^* \leq 1$	$\theta < \beta_1 C_1^*$	$e_1 = 0$
	$\theta \geq \beta_1 C_1^*$	$e_1 = 1$
$C_2^* \leq 1$	$\theta \leq \beta_1 C_1^* + \beta_2 C_2^*$	$e_2 = \theta / (\beta_1 C_1^* + \beta_2 C_2^*)$
	$\theta \geq \beta_1 C_1^* + \beta_2 C_2^*$	$e_2 = 1$
$C_1^* \geq 1$	$\theta < \beta_1 C_1^*$	$e_1 = 0$
	$\beta_1 C_1^* \leq \theta \leq \beta_2 + [\beta_1 C_1^* (1 + C_2^*) / C_2^*]$	$e_1 = \frac{1 - C_1^*}{[1 - (C_1^*/C_2^*)]}$
$C_2^* \geq 1$	$\theta \geq \beta_2 + [\beta_1 C_1^* (1 + C_2^*) / C_2^*]$	$e_1 = 1$
	$\theta \leq \beta_2 + (\beta_1 C_1^* / C_2^*)$	$e_2 = C_2^* \theta / (\beta_1 C_1^* + \beta_2 C_2^*)$
	$\theta > \beta_2 + (\beta_1 C_1^* / C_2^*)$	$e_2 = 1$
$C_1^* \geq 1$	all θ	e_1 is undefined
	$\theta \leq \beta_1 + (\beta_2 C_2^* / C_1^*)$	$e_2 = C_1^* \theta / (\beta_1 C_1^* + \beta_2 C_2^*)$
$C_2^* \leq C_1^*$	$\theta \geq \beta_1 + (\beta_2 C_2^* / C_1^*)$	$e_2 = 1$
	$\theta \leq \beta_1 C_1^* + n[\beta_2 + (\beta_1 C_1^* / C_2^*)]$	$e_1 = 0^a$
$C_1^* \geq 1$	$\beta_1 C_1^* + n[\beta_2 + (\beta_1 C_1^* / C_2^*)] \leq \theta \leq \beta_1 C_1^* + (n+1)[\beta_2 + (\beta_1 C_1^* / C_2^*)]$	$e_1 = \frac{C_1^*}{C_2^*} \left(n + \frac{1 - C_1^*}{1 - (C_1^*/C_2^*)} \right)$
	$\theta \geq \beta_1 C_1^* + (n+1)[\beta_2 + (\beta_1 C_1^* / C_2^*)]$	$e_1 = 1$
$C_2^* \geq C_1^*$	$\theta \leq \beta_2 + (\beta_1 C_1^* / C_2^*)$	$e_2 = C_2^* \theta / (\beta_1 C_1^* + \beta_2 C_2^*)$
	$\theta \geq \beta_2 + (\beta_1 C_1^* / C_2^*)$	$e_2 = 1$

^a n is integer such that $n - 1 < \frac{C_1^* - 1}{1 - (C_1^*/C_2^*)} \leq n$

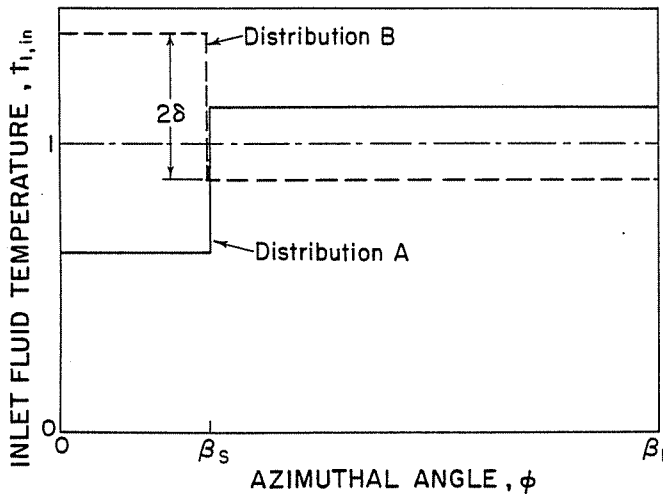


Fig. 4 Temperature distributions of period 1 inlet fluid used in analysis of nonuniform inlet temperatures

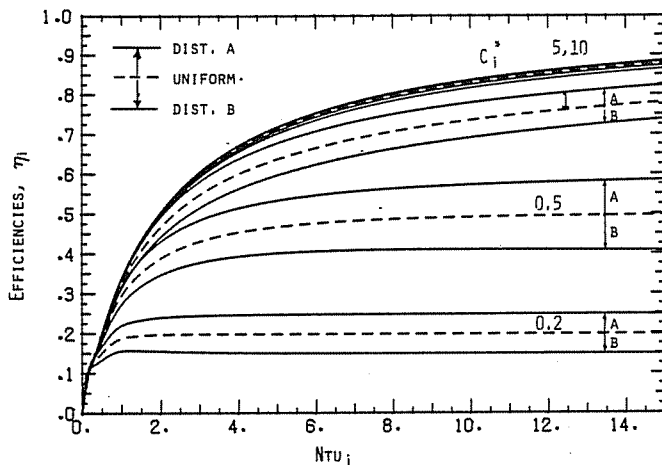


Fig. 5 Regenerator efficiency for nonuniform inlet conditions with $\beta_s = 0.5\beta_1$, $\delta = 0.25$, $Ntu_1 = Ntu_2$, $C_1^* = C_2^*$

1 matrix and fluid states are unchanged, while the period 2 transient response has continued its linear increase to $e_2 = 0.75$. The distribution within the matrix in period 2 shows that the equilibrium temperature profile is developing while pushing the lingering transient effects toward the period 2 outlet. At $\theta = 0.8$, all transient effects have been eliminated and the regenerator has reached periodic steady-state operation with $e_1 = 1$ and $e_2 = 1$.

This type of analysis has been performed for the general case of an unbalanced, asymmetric regenerator. The results are presented in Table 2.

The results of these equilibrium analyses define the values of η_i and e_i obtainable from a regenerator operating with infinite heat transfer coefficients. The results of the numerical analysis will show that these limits are approached for large values of Ntu . However, the main value of the analysis lies in the conceptualization of the heat transfer process in terms of a wave of temperature change which propagates through the regenerator with time. The insight gained from this analysis is used to explain the results obtained from the numerical and experimental investigations.

Numerical Analysis. The numerical analysis considers a regenerator with finite heat transfer coefficients as opposed to the infinite transfer coefficients assumed in the equilibrium analysis. The effect of finite transfer coefficients is to broaden, or smear, the equilibrium wavefront as it propagates through the matrix. The sharp wave fronts of Fig. 2 would

appear as an expanding fan, with the temperature increasing continuously on both sides of its center.

A regenerator with finite transfer coefficients is described by equations (3) and (4) with their associated boundary and initial conditions. Unfortunately, these equations cannot be solved analytically. Coppage and London [15] review some of the early approximate methods of analysis, most of which apply graphical and analytical techniques to a simplified problem. Lambertson [2] provided the first comprehensive set of solutions using finite difference techniques. Maclaine-cross [11] modified Lambertson's techniques and expanded the range of parameter values. The methods of solution employed in this paper are based on those of Lambertson and Maclaine-cross.

Numerical analysis results have been obtained for steady periodic operation with the inlet fluid temperature distributions shown in Fig. 4, where β_s and δ are parameters describing the distributions. The period 2 inlet fluid temperature has been assumed uniform at zero, and the period 1 inlet fluid temperature is such that $t_{1,in} = 1$. For each value of β_s , two distributions, which are reflections of each other about the mean of unity, are used. Distribution A will increase the regenerator efficiency since it exposes the matrix to a higher temperature just before it rotates into the period 2 fluid stream, resulting in a higher period 2 outlet fluid temperature. Similarly, distribution B will reduce the efficiency by exactly the same amount.

Figure 5 gives results as a function of Ntu_i for several values of C_i^* , with $Ntu_1 = Ntu_2$, $C_1^* = C_2^*$, $\delta = 0.5$ and $\beta_s = 0.5\beta_1$. These results show that the effect of inlet fluid temperature nonuniformities depends strongly on the matrix to fluid capacity rate ratios. For $C_i^* \geq 10$, nonuniformities have very little effect on regenerator efficiency. However, for $C_i^* \leq 1$, the effect is very pronounced. The difference between the regenerator efficiency with nonuniform inlet temperatures and that with uniform inlet temperatures will increase as δ increases. Table 1 shows that the equilibrium theory predicts $\eta_i = 1.0$ when $C_i^* \geq 1$, $\eta_i = 0.625$ when $C_i^* = 0.5$ and $\eta_i = 0.25$ when $C_i^* = 0.2$, for inlet temperature distribution A of this type. These predictions are seen to be close for small C_i^* values, even at low Ntu_i values.

The numerical analysis of a regenerator operating with a temporal step change in period 1 inlet fluid temperature is similar to that for a regenerator operating under periodic steady-state conditions. The transient response e_i is calculated from equation (10) using the computed time variation of the spatial average outlet fluid temperature. The outlet fluid temperatures for the initial and final steady periodic conditions are predetermined.

Results of the transient numerical analysis are presented in Figs. 6 and 7. Figure 6 shows the period 1 and period 2 transient responses for a balanced and symmetric regenerator with $C_i^* = 0.2$ and $C_i^* = 10$ for a range of values of Ntu_i . When $C_i^* = 0.2$, the results of the numerical analysis approach those of the equilibrium analysis, Table 2, as Ntu_i increases. When $C_i^* = 10$, the period 2 response e_2 also approaches the equilibrium analysis result of Table 2 as Ntu_i increases. While e_1 is undefined for $C_i^* > 1$ in the equilibrium analysis, it appears to approach zero with increasing Ntu_i . The results when $C_i^* = 10$ show good agreement with those of London et al. [5].

Figure 7 shows some unexpected effects of C_i^* on the transient response for a balanced and symmetric regenerator with $Ntu_i = 16$. From $C_i^* = 0.8$ to $C_i^* = 4$, the transient response, particularly e_1 , exhibits a periodicity with time having a wavelength approximately equal to the rotation period. This behavior is in dramatic contrast to both the predictions of the equilibrium theory, which compare well with the numerical results at both small and large values of C_i^* and the results presented in the literature [3, 5-9]. In fact, the periodicity is inherent to the transient operation of a rotary

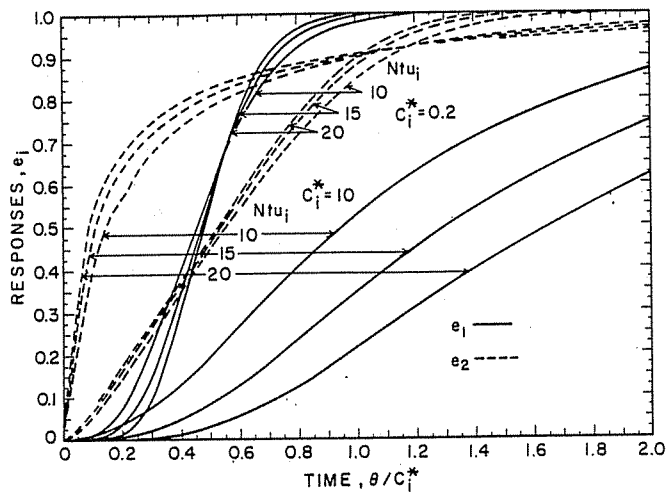


Fig. 6 Transient response of a balanced and symmetric regenerator

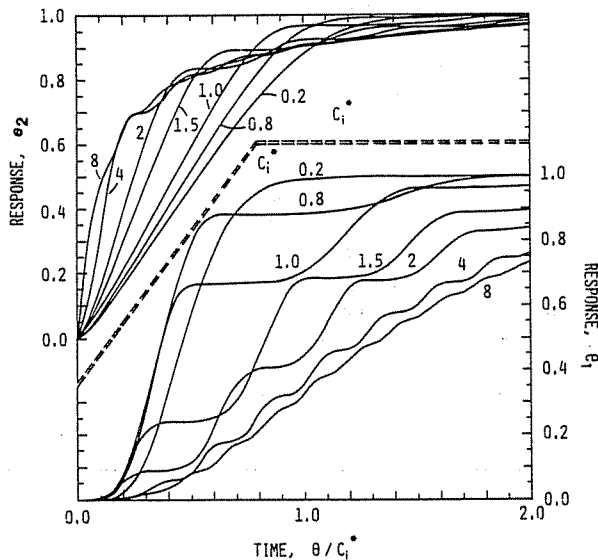


Fig. 7 Effect of C_1^* on regenerator transient response for $Ntu_1 = Ntu_2 = 16$ with $C_1 = C_2$

regenerator and is present at all but the smallest values of C_1^* . For large C_1^* , the amplitude and wavelength are small and the response approaches a monotonic increase with time.

The periodic behavior observed in Fig. 7 is due to the effects of finite transfer coefficients and the definition of the transient response as an indicator of the variation in the average fluid outlet temperature with time. Since the transient response represents an instantaneous measure of the outlet fluid temperatures, it reflects not only the changes from one rotation of the matrix to the next, but also the changes due to the propagation of temperature change waves during a single matrix rotation. In the case of infinite transfer coefficients, a balanced regenerator reaches steady-state operation with one rotation of the matrix; and the response is determined by the effects of the change waves on the outlet temperatures during that single matrix rotation. In the case of finite transfer coefficients, several matrix rotations are required to achieve steady-state operation. The overall trend toward steady-state operation is constructed from a series of smaller increases in the response caused by waves of temperature change which emerge at the fluid outlet with each successive rotation of the matrix.

The effects of finite transfer coefficients can be explained in terms of the shape of the temperature change wavefront. When $Ntu_1 = \infty$, temperature changes propagate through the matrix in the form of a sharp wavefront, and the fluid temperature is equal to the matrix temperature at every position. As Ntu_1 decreases, the wavefront broadens with time and distance, and the change in matrix temperature lags that of the fluid temperature. Both of these phenomena cause a "trapping" of the wavefront in the matrix, resulting in periodic increases in the transient response. At low values of C_1^* , both the matrix and fluid temperature wavefronts emerge from the matrix during the first period despite being broadened. However, as C_1^* increases, the trailing end of both the fluid and matrix temperature waves are trapped within the regenerator and are exposed to the period 2 fluid. Part of the wavefronts will then emerge with part of them again being exposed to the period 1 fluid. As a result, the transient response does not increase monotonically as for the equilibrium analysis, but increases in steps with each rotation of the matrix.

Figure 8 illustrates this effect using a quasi-equilibrium analysis in which the matrix temperature is assumed to equal

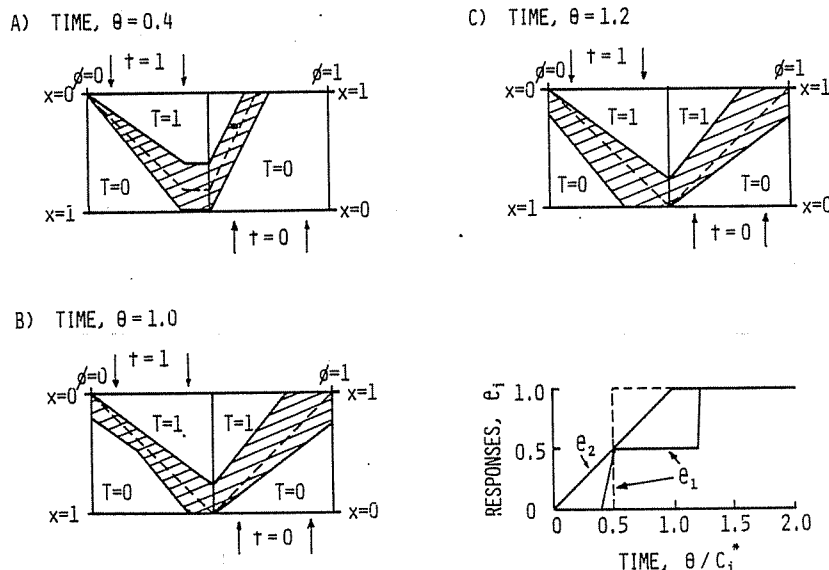


Fig. 8 Quasi-equilibrium analysis of transient response, with equilibrium analysis shown in dashed lines. The coordinate x increases in flow direction in each period. Variation of the transient responses with time is shown.

Table 3 Comparison of numerical and experimental results for nonuniform inlet temperatures

C_2^*/C_1^*	Ntu_1	C_1^*	$\eta_{1,num}$	$\Delta\eta_{1,num}$	$\eta_{1,exp}$	$\Delta\eta_{1,exp}$	Dist. Fig. 4
0.52	21.8	1.08	0.905	0.037	0.796	0.060	A
						0.046	B
0.52	21.8	5.08	0.996	0.000	0.968	0.004	A
						0.000	B
0.52	21.8	19.08	0.997	0.000	0.976	0.002	A
						0.001	B
0.98	21.0	1.04	0.829	0.049	0.758	0.053	A
						0.050	B
0.98	21.0	5.06	0.916	0.011	0.884	0.011	A
						0.009	B
0.98	21.0	19.01	0.927	0.004	0.898	0.007	A
						0.005	B
1.02	11.6	0.57	0.561	0.113	0.497	0.097	A
						0.099	B
1.02	11.6	3.03	0.831	0.023	0.811	0.031	A
						0.022	B
1.02	11.6	10.05	0.844	0.008	0.825	0.002	A
						0.003	B
2.05	11.4	0.56	0.456	0.098	0.434	0.095	A
						0.097	B
2.05	11.4	3.00	0.475	0.038	0.469	0.033	A
						0.042	B
2.05	11.4	10.03	0.489	0.014	0.472	0.020	A
						0.014	B

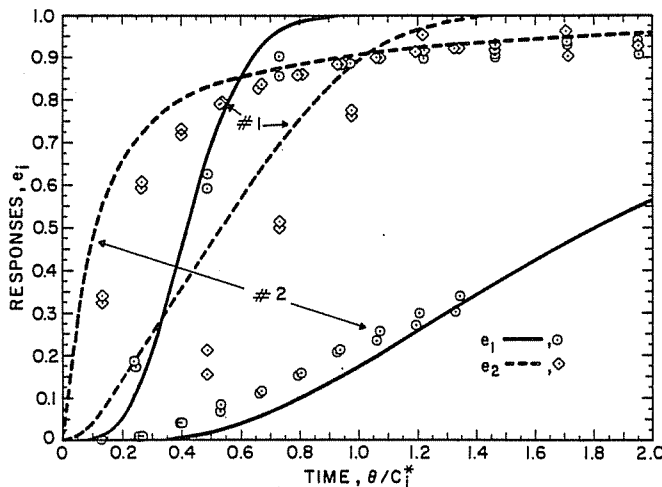


Fig. 9 Comparison of numerical and experimental results for transient inlet conditions. #1: $Ntu_1 = 12.2, C_1^* = 0.59, C_2^*/C_1^* = Ntu_2/Ntu_1 = 0.89$. #2: $Ntu_1 = 22.4, C_1^* = 20.1, C_2^*/C_1^* = Ntu_2/Ntu_1 = 0.98$.

the fluid temperature at every position, while the width of the wavefront increases linearly with time and distance about an average matrix to fluid capacity rate ratio of $C_1^* = 1$. At $\theta = 0.4$, the leading edge of the wave has just emerged from period 1, while the remainder is about to enter period 2. At $\theta = 1.0$, part of the wavefront has emerged from period 2, while the distribution in period 1 is already being affected by the trapped wavefront. Notice, though, that the period 1 outlet state remains constant until the effect of this trapped wavefront has propagated through period 1 of the matrix. When $\theta = 1.2$, the trapped part of the wavefront has emerged from period 1 and the regenerator has reached steady state. Under these assumptions, e_2 increases linearly while e_1 increases in two steps. In reality, this periodicity will be accentuated by the fact that the matrix temperature change lags that of the fluid.

Experimental Analysis

An experimental analysis of a regenerator operating with either nonuniform or transient inlet conditions was un-

dertaken to substantiate the predictions of the theoretical models. The experimental work for this investigation was performed on a regenerator test apparatus located at the CSIRO Division of Mechanical Engineering, now the CSIRO Division of Energy Technology. The apparatus, described in [16] and the Appendix, allows testing of a symmetric regenerator in countercurrent flow conditions.

Experimental tests of the regenerator operating under nonuniform inlet conditions were performed for two values of fluid velocity v_1 , two values of v_2 , and three different rotation speeds, for both distribution A and distribution B of Fig. 4 with $\beta_s = 0.5\beta_1$. Table 3 shows a comparison of the experimental results with those of the numerical model, for several of these steady state tests. In this table, $\Delta\eta_1$ is defined as the magnitude of the difference between the efficiency with nonuniform inlet conditions and that with uniform inlet conditions. The values of η_1 presented are the efficiencies with uniform inlet conditions. The results justify the main conclusion of the numerical analysis that nonuniform inlet temperatures have little effect on the performance of a regenerator operating with large matrix to fluid capacity rate ratios. As the capacity rate ratio decreases, though, the effect becomes substantially more significant.

Experimental tests of the regenerator exposed to a temporal step change in hot side inlet fluid temperature were also performed for two values of v_1 , two values of v_2 , and three different rotation speeds. The regenerator was first brought to periodic steady-state conditions and then exposed to a step change in the hot side fluid temperature using a fast-response heater.

Comparisons between the numerical and experimental results for the regenerator exposed to a temporal step change in inlet fluid temperature are shown in Figs. 9 and 10. For these comparisons, the numerical results were calculated using the actual increase in the hot side fluid temperature obtained from the experiment, rather than the step increase assumed in the mathematical model. Use of the actual temperature rise causes a slight delay in the response e_2 , particularly at low values of C_1^* . Figure 9 shows comparisons for two different set of parameters: Test 1 corresponds to $Ntu_1 = 12.2, C_1^* = 0.59$, and $C_2^*/C_1^* = Ntu_2/Ntu_1 = 0.89$, and Test 2 corresponds to $Ntu_1 = 22.4, C_1^* = 20.1$, and $C_2^*/C_1^* = Ntu_2/Ntu_1 = 0.98$. The data points correspond to replicated experimental tests. The

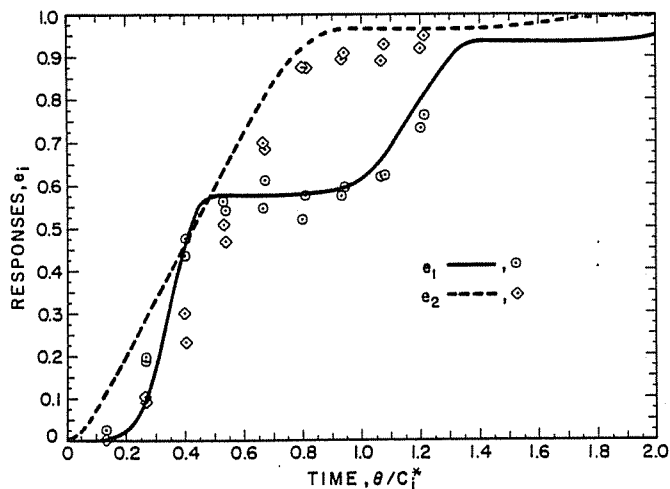


Fig. 10 Comparison of numerical and experimental results for transient inlet conditions with $Ntu_1 = 22.4$, $C_1^* = 1.1$, $C_2^*/C_1^* = Ntu_2/Ntu_1 = 0.98$

differences between the data points of these replicates provide an indication of the precision of the experiment. The results generally show good agreement, although the period 2 response of the experimental tests lags that of the numerical analysis for a short time after the temperature change. This lag in response is attributed to the thermal capacity of the rotor apart from the porous matrix and the transit time of the rotor in the diametral seals. For the small matrix to fluid capacity rate ratio of Test 1, the period 1 response e_1 increases slightly more rapidly than that of period 2, e_2 . However for the high capacity rate ratio of Test 2, e_2 responds much more quickly than e_1 . Figure 10 presents Test 3 with $Ntu_1 = 22.4$, $C_1^* = 1.1$, and $C_2^*/C_1^* = Ntu_2/Ntu_1 = 0.98$. Both the numerical and experimental results dramatically illustrate the periodic nature of the regenerator response in this regime of matrix to fluid capacity rate ratios.

Conclusions

The investigation of a counterflow, balanced, and symmetric rotary heat exchanger operating under periodic steady-state conditions with circumferentially nonuniform inlet conditions has led to the following major conclusions.

1 At large matrix to fluid capacity rate ratios, associated with high effectiveness heat exchangers, nonuniformities in inlet fluid temperatures have little effect on steady-state regenerator performance. Under these operating conditions, the amount of heat transferred between the two fluid streams depends on the average energy levels of the two streams.

2 At small matrix to fluid capacity rate ratios, which occur in the analysis of heat and mass regenerators, inlet fluid temperature nonuniformities can have a substantial effect on the steady-state performance. This performance can often be predicted by the equilibrium analysis, even at low values of Ntu_i . The regenerator efficiency is increased by nonuniformities of the form of distribution A as shown in Fig. 4 and decreased by nonuniformities of the form of distribution B. Under these operating conditions, the amount of heat transferred between the two fluid streams depends not only on the average energy levels of the two streams, but also on the distribution of that energy within the streams. If this distribution can be varied, it can be optimized to either maximize or minimize the energy transfer. Similarly, by considering the inlet temperature as a design variable, the same level of performance can be achieved by regenerators with considerably different values of Ntu_i and C_i^* .

The investigation of the transient response of a counterflow, balanced, and symmetric regenerator exposed to a

transient step change in fluid inlet temperature has produced the following major conclusions.

1 At large matrix to fluid capacity rate ratios, results and conclusions concur with those of London et al. [5] and Willmott and Burns [7]. The period 2 outlet fluid responds much more quickly than the period 1 fluid, and both respond monotonically with time.

2 At small matrix to fluid capacity rate ratios, the results show little sensitivity to Ntu_i and are generally determined by C_i^* . The period 1 outlet fluid responds slightly more rapidly than the period 2 fluid, and both respond monotonically with time. The equilibrium analysis provides a reasonable approximation to regenerator performance, even at low values of Ntu_i .

3 At intermediate values of the matrix to fluid capacity rate ratios, the transient responses exhibit periodicity in time, with the responses increasing in steps with each rotation of the matrix. The effect is most pronounced between $C_i^* = 0.7$ and $C_i^* = 2$, though extending through $C_i^* = 8$. The periodicity is explained by the effects of finite transfer coefficients and the definition of the transient response, and is substantiated by experimental results.

Acknowledgments

The work presented here was sponsored by the U.S. Department of Energy through a contract to the University of Wisconsin for the study of solar desiccant cooling systems (Contract DEAC03-79SF10548), with the experimental work subcontracted to the CSIRO Division of Mechanical Engineering, now the CSIRO Division of Energy Technology.

The authors are very grateful for the assistance of colleagues at the University of Wisconsin Solar Energy Laboratory and the CSIRO Division of Mechanical Engineering. Mr. W. M. J. Ellul at CSIRO was particularly helpful in the experimental work of this paper. Professor J. W. Mitchell of the University of Wisconsin provided much of the initial stimulus for this work and gave valuable advice on the interpretation of the results. The suggestions of Dr. I. L. Maclaine-cross of the University of New South Wales, Australia, were also very helpful.

References

- 1 Hausen, H., "On The Theory of Heat Exchange in Regenerators," *Zeitschrift fuer Angewandte Mathematik und Mechanik*, Vol. 9, 1929, pp. 173-200.
- 2 Lambertson, T. J., "Performance Factors of a Periodic-Flow Heat Exchanger," *ASME Transactions*, Vol. 80, 1958, pp. 586-592.
- 3 Kays, W. M., and London, A. L., *Compact Heat Exchangers*, 2d ed., McGraw Hill, New York, 1964.
- 4 Shah, R. K., "Thermal Design Theory for Regenerators," *Heat Exchangers: Thermal-Hydraulic Fundamentals and Design*, edited by S. Kakac, A. E. Bergles, and F. Mayinger, Hemisphere/McGraw-Hill, Washington, D.C., 1981, pp. 721-763.
- 5 London, A. L., Sampson, D. F., and McGowan, J. G., "The Transient Response of Gas Turbine Plant Heat Exchangers-Additional Solutions for Regenerators of the Periodic-Flow and Direct-Transfer Type," *ASME Journal of Engineering for Power*, Vol. 86, Apr. 1964, pp. 127-135.
- 6 Chao, W. W., "Research and Development of an Experimental Rotary Regenerator for Automotive Gas Turbines," *Proceedings American Power Conference*, Vol. 17, 1955, pp. 358-374.
- 7 Willmott, A. J., and Burns, A., "Transient Response of Periodic Flow Regenerators," *International Journal of Heat and Mass Transfer*, Vol. 20, 1977, pp. 753-761.
- 8 Schmidt, F. W., and Willmott, A. J., *Thermal Energy Storage and Regeneration*, ch. 10, Hemisphere/McGraw-Hill, Washington, D.C., 1981, pp. 219-242.
- 9 Shah, R. K., "Transient Response of Heat Exchangers," *Heat Exchangers: Thermal-Hydraulic Fundamentals and Design*, edited by S. Kakac, A. E. Bergles, and F. Mayinger, Hemisphere/McGraw-Hill, Washington, D.C., 1981, pp. 915-953.
- 10 Maclaine-cross, I. L., and Banks, P. J., "Coupled Heat and Mass Transfer in Regenerators-Predictions Using an Analogy with Heat Transfer," *International Journal of Heat and Mass Transfer*, Vol. 15, 1972, pp. 1225-1242.

11 Maclaine-cross, I. L., "A Theory of Combined Heat and Mass Transfer in Regenerators," Ph.D. thesis, Monash University, Melbourne, 1974.

12 Banks, P. J., "Prediction of Heat and Water Vapour Exchanger Performance from that of a Similar Heat Exchanger," *Compact Heat Exchangers—History, Technological Advancement, and Mechanical Design Problems*, edited by R. K. Shah, C. F. McDonald, and C. P. Howard, Book No. G00183, HTD-Vol. 10, ASME, New York, 1980, pp. 57-64.

13 Cassie, A. B. D., "Adsorption of Water Vapor by Wool Fibers. Part II—Theory of Propagation of Temperature Change," *Transactions of the Faraday Society*, Vol. 36, 1940, pp. 453-465.

14 Lighthill, M. J., and Whitham, G. B., "On Kinematic Waves," *Proceedings of the Royal Society of London*, Vol. A229, 1955, pp. 281-345.

15 Coppage, J. E. and London, A. L., "The Periodic-Flow Regenerator—A Summary of Design Theory," *ASME Transactions*, Vol. 75, July 1953, pp. 779-787.

16 Dunkle, R. V., Banks, P. J., and Ellul, W. M. J., "Regenerator Research, Development, and Applications in Australia—1978 Status," *International Journal of Refrigeration*, Vol. 1, No. 3, Sept. 1978, pp. 143-150.

17 Dunkle, R. V. and Maclaine-cross, I. L., "Theory and Design of Rotary Heat Exchangers for Air Conditioning," *Mechanical and Chemical Engineering, Transactions of The Institution of Engineers, Australia*, Vol. MC6, No. 1, May 1970, pp. 1-6.

18 Dunkle, R. V., Banks, P. J., and Maclaine-cross, I. L., "Wound Parallel Plate Exchangers for Air-Conditioning Applications," *Compact Heat Exchangers—History, Technological Advancement and Mechanical Design Problems*, edited by R. K. Shah, C. F. McDonald, and C. P. Howard, Book No. G00183, HTD-Vol. 10, ASME, New York, 1980, pp. 65-71.

APPENDIX

The basic experimental apparatus used for this investigation is described in [16]. Four modifications were made to this apparatus to allow testing for the desired results: a new regenerator was constructed, a fast-response split-duct heater was designed and constructed, the temperature measuring devices were replaced, and the duct configuration was modified.

The regenerator was constructed by spirally winding a polyester film around an aluminum hub [17, 18]. The spirals are separated by aluminum spacers held in spokes to produce parallel flow passages. The polyester film is 0.125 mm thick and the flow passages are 0.914 mm wide giving a matrix porosity to air flow of 88 percent. The regenerator has a length of 160 mm and an effective cross-sectional area of

0.0935 m² per period. The properties of the matrix are such that the conductivity assumptions of the theoretical model are justified. The polyester film is thin enough that axial conduction effects are negligible and the resistance to heat transfer into the film at any position is small compared to the matrix-fluid convective transfer resistance. Airflow through the matrix was at a Reynolds number of the order of 100, so that the convective transfer coefficient for the numerical model was predicted assuming laminar flow [3, 17].

A fast-response, split-duct heater was designed to balance the trade-offs between rapid heater response, low heater wire temperature, and high power output. The heater has a response time of approximately 5 s and a power output of up to 3.6 kW. It is constructed to provide spatial nonuniformities as in Fig. 4 with $\beta_s = 0.5\beta_1$.

Thermocouple grids are located immediately upstream and downstream of the regenerator in each flow stream, which allows measurement of both spatial average temperatures and temperature distributions. The error in temperature measurement including radiation effects, is estimated to be 2 percent of the total temperature difference across the regenerator.

The ductwork was modified to allow testing of a regenerator operating under unbalanced flow conditions. The flow rates of the two fluid streams are controlled by separate fans. Flow nozzles are located in each fluid stream, measuring flow rates to within an estimated error tolerance of 1.8 percent. At the regenerator, the two fluid streams are separated by clearance seals, with an average clearance of 1.1 mm. Corrections for the effects of fluid stream mixing due to leakage are made as in [17].

Preliminary tests indicated that the velocity was uniform to within ± 10 percent with the regenerator removed. Since the matrix forms the largest flow resistance in each stream, the uniformity of the distributions was expected to improve with the regenerator in place. The temperature distribution with the matrix in position was uniform to within ± 3 percent, implying similar uniformity of velocity. Analyses of the regenerator operating under steady periodic conditions showed conservation of energy to within 5 percent.

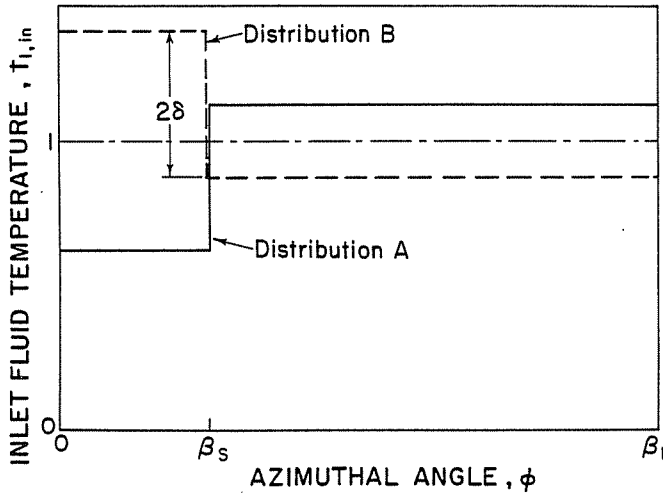


Fig. 4 Temperature distributions of period 1 inlet fluid used in analysis of nonuniform inlet temperatures

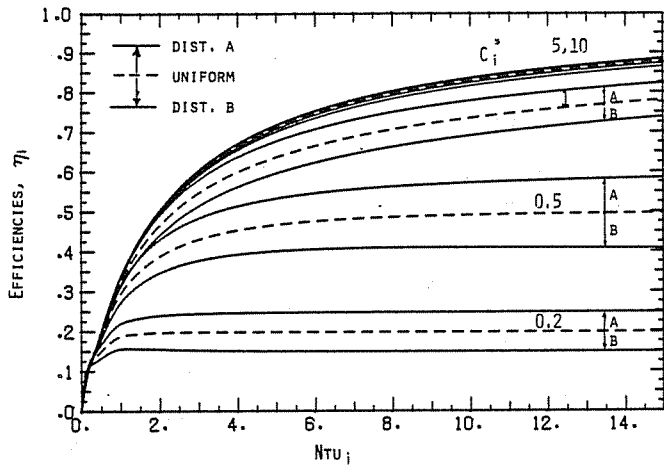


Fig. 5 Regenerator efficiency for nonuniform inlet conditions with $\beta_s = 0.5\beta_1$, $\delta = 0.25$, $Ntu_1 = Ntu_2$, $C_1 = C_2$

1 matrix and fluid states are unchanged, while the period 2 transient response has continued its linear increase to $e_2 = 0.75$. The distribution within the matrix in period 2 shows that the equilibrium temperature profile is developing while pushing the lingering transient effects toward the period 2 outlet. At $\theta = 0.8$, all transient effects have been eliminated and the regenerator has reached periodic steady-state operation with $e_1 = 1$ and $e_2 = 1$.

This type of analysis has been performed for the general case of an unbalanced, asymmetric regenerator. The results are presented in Table 2.

The results of these equilibrium analyses define the values of η_i and e_i obtainable from a regenerator operating with infinite heat transfer coefficients. The results of the numerical analysis will show that these limits are approached for large values of Ntu . However, the main value of the analysis lies in the conceptualization of the heat transfer process in terms of a wave of temperature change which propagates through the regenerator with time. The insight gained from this analysis is used to explain the results obtained from the numerical and experimental investigations.

Numerical Analysis. The numerical analysis considers a regenerator with finite heat transfer coefficients as opposed to the infinite transfer coefficients assumed in the equilibrium analysis. The effect of finite transfer coefficients is to broaden, or smear, the equilibrium wavefront as it propagates through the matrix. The sharp wave fronts of Fig. 2 would

appear as an expanding fan, with the temperature increasing continuously on both sides of its center.

A regenerator with finite transfer coefficients is described by equations (3) and (4) with their associated boundary and initial conditions. Unfortunately, these equations cannot be solved analytically. Coppage and London [15] review some of the early approximate methods of analysis, most of which apply graphical and analytical techniques to a simplified problem. Lambertson [2] provided the first comprehensive set of solutions using finite difference techniques. Maclaine-cross [11] modified Lambertson's techniques and expanded the range of parameter values. The methods of solution employed in this paper are based on those of Lambertson and Maclaine-cross.

Numerical analysis results have been obtained for steady periodic operation with the inlet fluid temperature distributions shown in Fig. 4, where β_s and δ are parameters describing the distributions. The period 2 inlet fluid temperature has been assumed uniform at zero, and the period 1 inlet fluid temperature is such that $t_{1,in} = 1$. For each value of β_s , two distributions, which are reflections of each other about the mean of unity, are used. Distribution A will increase the regenerator efficiency since it exposes the matrix to a higher temperature just before it rotates into the period 2 fluid stream, resulting in a higher period 2 outlet fluid temperature. Similarly, distribution B will reduce the efficiency by exactly the same amount.

Figure 5 gives results as a function of Ntu_i for several values of C_i^* , with $Ntu_1 = Ntu_2$, $C_1^* = C_2^*$, $\delta = 0.5$ and $\beta_s = 0.5\beta_1$. These results show that the effect of inlet fluid temperature nonuniformities depends strongly on the matrix to fluid capacity rate ratios. For $C_i^* \geq 10$, nonuniformities have very little effect on regenerator efficiency. However, for $C_i^* \leq 1$, the effect is very pronounced. The difference between the regenerator efficiency with nonuniform inlet temperatures and that with uniform inlet temperatures will increase as δ increases. Table 1 shows that the equilibrium theory predicts $\eta_i = 1.0$ when $C_i^* \geq 1$, $\eta_i = 0.625$ when $C_i^* = 0.5$ and $\eta_i = 0.25$ when $C_i^* = 0.2$, for inlet temperature distribution A of this type. These predictions are seen to be close for small C_i^* values, even at low Ntu_i values.

The numerical analysis of a regenerator operating with a temporal step change in period 1 inlet fluid temperature is similar to that for a regenerator operating under periodic steady-state conditions. The transient response e_i is calculated from equation (10) using the computed time variation of the spatial average outlet fluid temperature. The outlet fluid temperatures for the initial and final steady periodic conditions are predetermined.

Results of the transient numerical analysis are presented in Figs. 6 and 7. Figure 6 shows the period 1 and period 2 transient responses for a balanced and symmetric regenerator with $C_1^* = 0.2$ and $C_2^* = 10$ for a range of values of Ntu_i . When $C_1^* = 0.2$, the results of the numerical analysis approach those of the equilibrium analysis, Table 2, as Ntu_i increases. When $C_2^* = 10$, the period 2 response e_2 also approaches the equilibrium analysis result of Table 2 as Ntu_i increases. While e_1 is undefined for $C_i^* > 1$ in the equilibrium analysis, it appears to approach zero with increasing Ntu_i . The results when $C_2^* = 10$ show good agreement with those of London et al. [5].

Figure 7 shows some unexpected effects of C_i^* on the transient response for a balanced and symmetric regenerator with $Ntu_i = 16$. From $C_1^* = 0.8$ to $C_1^* = 4$, the transient response, particularly e_1 , exhibits a periodicity with time having a wavelength approximately equal to the rotation period. This behavior is in dramatic contrast to both the predictions of the equilibrium theory, which compare well with the numerical results at both small and large values of C_i^* and the results presented in the literature [3, 5-9]. In fact, the periodicity is inherent to the transient operation of a rotary

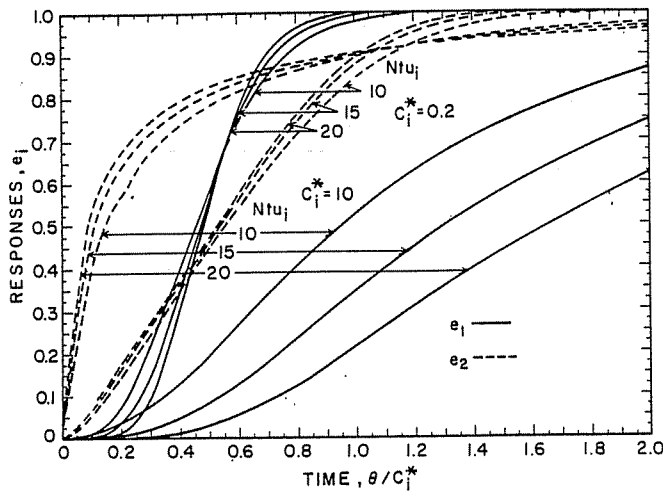


Fig. 6 Transient response of a balanced and symmetric regenerator

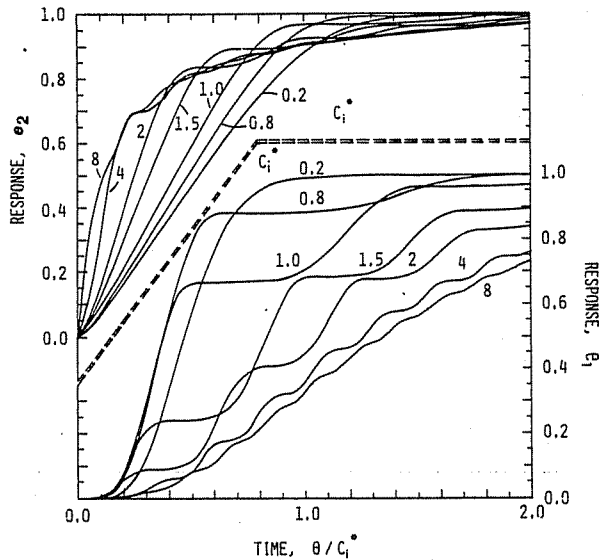


Fig. 7 Effect of C_1^* on regenerator transient response for $Ntu_1 = Ntu_2 = 16$ with $C_1 = C_2$

regenerator and is present at all but the smallest values of C_1^* . For large C_1^* , the amplitude and wavelength are small and the response approaches a monotonic increase with time.

The periodic behavior observed in Fig. 7 is due to the effects of finite transfer coefficients and the definition of the transient response as an indicator of the variation in the average fluid outlet temperature with time. Since the transient response represents an instantaneous measure of the outlet fluid temperatures, it reflects not only the changes from one rotation of the matrix to the next, but also the changes due to the propagation of temperature change waves during a single matrix rotation. In the case of infinite transfer coefficients, a balanced regenerator reaches steady-state operation with one rotation of the matrix; and the response is determined by the effects of the change waves on the outlet temperatures during that single matrix rotation. In the case of finite transfer coefficients, several matrix rotations are required to achieve steady-state operation. The overall trend toward steady-state operation is constructed from a series of smaller increases in the response caused by waves of temperature change which emerge at the fluid outlet with each successive rotation of the matrix.

The effects of finite transfer coefficients can be explained in terms of the shape of the temperature change wavefront. When $Ntu_i = \infty$, temperature changes propagate through the matrix in the form of a sharp wavefront, and the fluid temperature is equal to the matrix temperature at every position. As Ntu_i decreases, the wavefront broadens with time and distance, and the change in matrix temperature lags that of the fluid temperature. Both of these phenomena cause a "trapping" of the wavefront in the matrix, resulting in periodic increases in the transient response. At low values of C_1^* , both the matrix and fluid temperature wavefronts emerge from the matrix during the first period despite being broadened. However, as C_1^* increases, the trailing end of both the fluid and matrix temperature waves are trapped within the regenerator and are exposed to the period 2 fluid. Part of the wavefronts will then emerge with part of them again being exposed to the period 1 fluid. As a result, the transient response does not increase monotonically as for the equilibrium analysis, but increases in steps with each rotation of the matrix.

Figure 8 illustrates this effect using a quasi-equilibrium analysis in which the matrix temperature is assumed to equal

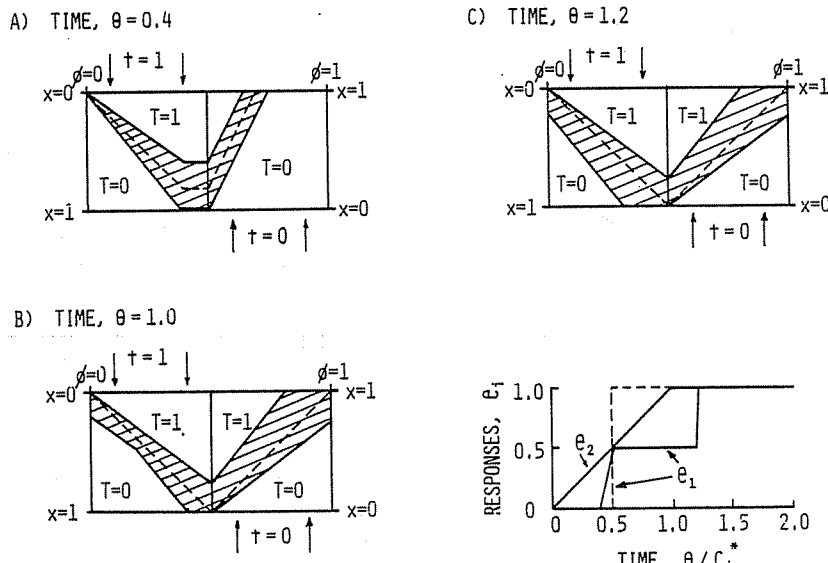


Fig. 8 Quasi-equilibrium analysis of transient response, with equilibrium analysis shown in dashed lines. The coordinate x increases in flow direction in each period. Variation of the transient responses with time is shown.

Table 3 Comparison of numerical and experimental results for nonuniform inlet temperatures

C_2^*/C_1^*	Ntu_1	C_1^*	$\eta_{1,num}$	$\Delta\eta_{1,num}$	$\eta_{1,exp}$	$\Delta\eta_{1,exp}$	Dist. Fig. 4
0.52	21.8	1.08	0.905	0.037	0.796	0.060	A
						0.046	B
0.52	21.8	5.08	0.996	0.000	0.968	0.004	A
						0.000	B
0.52	21.8	19.08	0.997	0.000	0.976	0.002	A
						0.001	B
0.98	21.0	1.04	0.829	0.049	0.758	0.053	A
						0.050	B
0.98	21.0	5.06	0.916	0.011	0.884	0.011	A
						0.009	B
0.98	21.0	19.01	0.927	0.004	0.898	0.007	A
						0.005	B
1.02	11.6	0.57	0.561	0.113	0.497	0.097	A
						0.099	B
1.02	11.6	3.03	0.831	0.023	0.811	0.031	A
						0.022	B
1.02	11.6	10.05	0.844	0.008	0.825	0.002	A
						0.003	B
2.05	11.4	0.56	0.456	0.098	0.434	0.095	A
						0.097	B
2.05	11.4	3.00	0.475	0.038	0.469	0.033	A
						0.042	B
2.05	11.4	10.03	0.489	0.014	0.472	0.020	A
						0.014	B

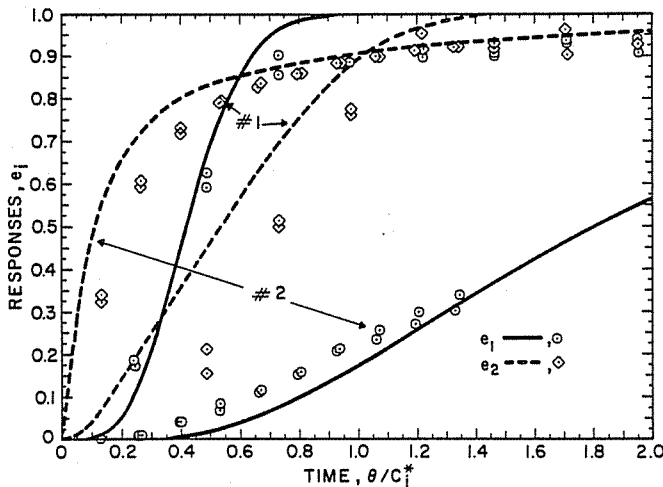


Fig. 9 Comparison of numerical and experimental results for transient inlet conditions. #1: $Ntu_1 = 12.2$, $C_1^* = 0.59$, $C_2^*/C_1^* = Ntu_2/Ntu_1 = 0.89$. #2: $Ntu_1 = 22.4$, $C_1^* = 20.1$, $C_2^*/C_1^* = Ntu_2/Ntu_1 = 0.98$.

the fluid temperature at every position, while the width of the wavefront increases linearly with time and distance about an average matrix to fluid capacity rate ratio of $C_1^* = 1$. At $\theta = 0.4$, the leading edge of the wave has just emerged from period 1, while the remainder is about to enter period 2. At $\theta = 1.0$, part of the wavefront has emerged from period 2, while the distribution in period 1 is already being affected by the trapped wavefront. Notice, though, that the period 1 outlet state remains constant until the effect of this trapped wavefront has propagated through period 1 of the matrix. When $\theta = 1.2$, the trapped part of the wavefront has emerged from period 1 and the regenerator has reached steady state. Under these assumptions, e_2 increases linearly while e_1 increases in two steps. In reality, this periodicity will be accentuated by the fact that the matrix temperature change lags that of the fluid.

Experimental Analysis

An experimental analysis of a regenerator operating with either nonuniform or transient inlet conditions was un-

dertaken to substantiate the predictions of the theoretical models. The experimental work for this investigation was performed on a regenerator test apparatus located at the CSIRO Division of Mechanical Engineering, now the CSIRO Division of Energy Technology. The apparatus, described in [16] and the Appendix, allows testing of a symmetric regenerator in countercurrent flow conditions.

Experimental tests of the regenerator operating under nonuniform inlet conditions were performed for two values of fluid velocity v_1 , two values of v_2 , and three different rotation speeds, for both distribution A and distribution B of Fig. 4 with $\beta_2 = 0.5\beta_1$. Table 3 shows a comparison of the experimental results with those of the numerical model, for several of these steady state tests. In this table, $\Delta\eta_1$ is defined as the magnitude of the difference between the efficiency with nonuniform inlet conditions and that with uniform inlet conditions. The values of η_1 presented are the efficiencies with uniform inlet conditions. The results justify the main conclusion of the numerical analysis that nonuniform inlet temperatures have little effect on the performance of a regenerator operating with large matrix to fluid capacity rate ratios. As the capacity rate ratio decreases, though, the effect becomes substantially more significant.

Experimental tests of the regenerator exposed to a temporal step change in hot side inlet fluid temperature were also performed for two values of v_1 , two values of v_2 , and three different rotation speeds. The regenerator was first brought to periodic steady-state conditions and then exposed to a step change in the hot side fluid temperature using a fast-response heater.

Comparisons between the numerical and experimental results for the regenerator exposed to a temporal step change in inlet fluid temperature are shown in Figs. 9 and 10. For these comparisons, the numerical results were calculated using the actual increase in the hot side fluid temperature obtained from the experiment, rather than the step increase assumed in the mathematical model. Use of the actual temperature rise causes a slight delay in the response e_2 , particularly at low values of C_1^* . Figure 9 shows comparisons for two different set of parameters: Test 1 corresponds to $Ntu_1 = 12.2$, $C_1^* = 0.59$, and $C_2^*/C_1^* = Ntu_2/Ntu_1 = 0.89$, and Test 2 corresponds to $Ntu_1 = 22.4$, $C_1^* = 20.1$, and $C_2^*/C_1^* = Ntu_2/Ntu_1 = 0.98$. The data points correspond to replicated experimental tests. The

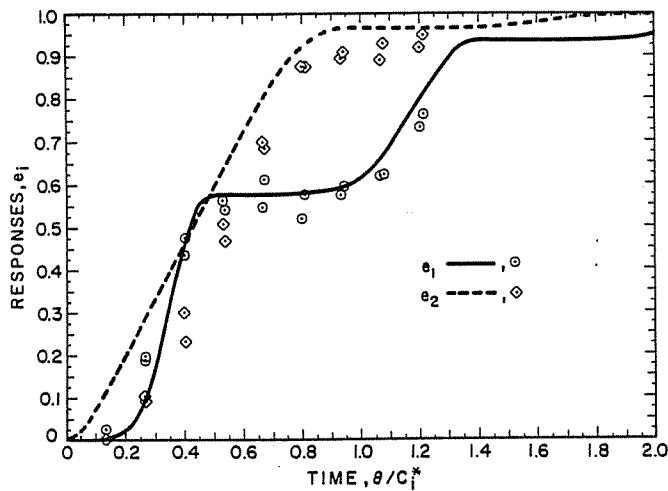


Fig. 10 Comparison of numerical and experimental results for transient inlet conditions with $Ntu_1 = 22.4$, $C_1^* = 1.1$, $C_2^*/C_1^* = Ntu_2/Ntu_1 = 0.98$

differences between the data points of these replicates provide an indication of the precision of the experiment. The results generally show good agreement, although the period 2 response of the experimental tests lags that of the numerical analysis for a short time after the temperature change. This lag in response is attributed to the thermal capacity of the rotor apart from the porous matrix and the transit time of the rotor in the diametral seals. For the small matrix to fluid capacity rate ratio of Test 1, the period 1 response e_1 increases slightly more rapidly than that of period 2, e_2 . However for the high capacity rate ratio of Test 2, e_2 responds much more quickly than e_1 . Figure 10 presents Test 3 with $Ntu_1 = 22.4$, $C_1^* = 1.1$, and $C_2^*/C_1^* = Ntu_2/Ntu_1 = 0.98$. Both the numerical and experimental results dramatically illustrate the periodic nature of the regenerator response in this regime of matrix to fluid capacity rate ratios.

Conclusions

The investigation of a counterflow, balanced, and symmetric rotary heat exchanger operating under periodic steady-state conditions with circumferentially nonuniform inlet conditions has led to the following major conclusions.

1 At large matrix to fluid capacity rate ratios, associated with high effectiveness heat exchangers, nonuniformities in inlet fluid temperatures have little effect on steady-state regenerator performance. Under these operating conditions, the amount of heat transferred between the two fluid streams depends on the average energy levels of the two streams.

2 At small matrix to fluid capacity rate ratios, which occur in the analysis of heat and mass regenerators, inlet fluid temperature nonuniformities can have a substantial effect on the steady-state performance. This performance can often be predicted by the equilibrium analysis, even at low values of Ntu_i . The regenerator efficiency is increased by nonuniformities of the form of distribution A as shown in Fig. 4 and decreased by nonuniformities of the form of distribution B. Under these operating conditions, the amount of heat transferred between the two fluid streams depends not only on the average energy levels of the two streams, but also on the distribution of that energy within the streams. If this distribution can be varied, it can be optimized to either maximize or minimize the energy transfer. Similarly, by considering the inlet temperature as a design variable, the same level of performance can be achieved by regenerators with considerably different values of Ntu_i and C_i^* .

The investigation of the transient response of a counterflow, balanced, and symmetric regenerator exposed to a

transient step change in fluid inlet temperature has produced the following major conclusions.

1 At large matrix to fluid capacity rate ratios, results and conclusions concur with those of London et al. [5] and Willmott and Burns [7]. The period 2 outlet fluid responds much more quickly than the period 1 fluid, and both respond monotonically with time.

2 At small matrix to fluid capacity rate ratios, the results show little sensitivity to Ntu_i and are generally determined by C_i^* . The period 1 outlet fluid responds slightly more rapidly than the period 2 fluid, and both respond monotonically with time. The equilibrium analysis provides a reasonable approximation to regenerator performance, even at low values of Ntu_i .

3 At intermediate values of the matrix to fluid capacity rate ratios, the transient responses exhibit periodicity in time, with the responses increasing in steps with each rotation of the matrix. The effect is most pronounced between $C_1^* = 0.7$ and $C_1^* = 2$, though extending through $C_1^* = 8$. The periodicity is explained by the effects of finite transfer coefficients and the definition of the transient response, and is substantiated by experimental results.

Acknowledgments

The work presented here was sponsored by the U.S. Department of Energy through a contract to the University of Wisconsin for the study of solar desiccant cooling systems (Contract DEAC03-79SF10548), with the experimental work subcontracted to the CSIRO Division of Mechanical Engineering, now the CSIRO Division of Energy Technology.

The authors are very grateful for the assistance of colleagues at the University of Wisconsin Solar Energy Laboratory and the CSIRO Division of Mechanical Engineering. Mr. W. M. J. Ellul at CSIRO was particularly helpful in the experimental work of this paper. Professor J. W. Mitchell of the University of Wisconsin provided much of the initial stimulus for this work and gave valuable advice on the interpretation of the results. The suggestions of Dr. I. L. Maclaine-cross of the University of New South Wales, Australia, were also very helpful.

References

- 1 Hausen, H., "On The Theory of Heat Exchange in Regenerators," *Zeitschrift fuer Angewandte Mathematik und Mechanik*, Vol. 9, 1929, pp. 173-200.
- 2 Lambertson, T. J., "Performance Factors of a Periodic-Flow Heat Exchanger," *ASME Transactions*, Vol. 80, 1958, pp. 586-592.
- 3 Kays, W. M., and London, A. L., *Compact Heat Exchangers*, 2d ed., McGraw Hill, New York, 1964.
- 4 Shah, R. K., "Thermal Design Theory for Regenerators," *Heat Exchangers: Thermal-Hydraulic Fundamentals and Design*, edited by S. Kakac, A. E. Bergles, and F. Mayinger, Hemisphere/McGraw-Hill, Washington, D.C., 1981, pp. 721-763.
- 5 London, A. L., Sampsel, D. F., and McGowan, J. G., "The Transient Response of Gas Turbine Plant Heat Exchangers-Additional Solutions for Regenerators of the Periodic-Flow and Direct-Transfer Type," *ASME Journal of Engineering for Power*, Vol. 86, Apr. 1964, pp. 127-135.
- 6 Chao, W. W., "Research and Development of an Experimental Rotary Regenerator for Automotive Gas Turbines," *Proceedings American Power Conference*, Vol. 17, 1955, pp. 358-374.
- 7 Willmott, A. J., and Burns, A., "Transient Response of Periodic Flow Regenerators," *International Journal of Heat and Mass Transfer*, Vol. 20, 1977, pp. 753-761.
- 8 Schmidt, F. W., and Willmott, A. J., *Thermal Energy Storage and Regeneration*, ch. 10, Hemisphere/McGraw-Hill, Washington, D.C., 1981, pp. 219-242.
- 9 Shah, R. K., "Transient Response of Heat Exchangers," *Heat Exchangers: Thermal-Hydraulic Fundamentals and Design*, edited by S. Kakac, A. E. Bergles, and F. Mayinger, Hemisphere/McGraw-Hill, Washington, D.C., 1981, pp. 915-953.
- 10 Maclaine-cross, I. L., and Banks, P. J., "Coupled Heat and Mass Transfer in Regenerators-Predictions Using an Analogy with Heat Transfer," *International Journal of Heat and Mass Transfer*, Vol. 15, 1972, pp. 1225-1242.

- 11 Maclaine-cross, I. L., "A Theory of Combined Heat and Mass Transfer in Regenerators," Ph.D. thesis, Monash University, Melbourne, 1974.
- 12 Banks, P. J., "Prediction of Heat and Water Vapour Exchanger Performance from that of a Similar Heat Exchanger," *Compact Heat Exchangers—History, Technological Advancement, and Mechanical Design Problems*, edited by R. K. Shah, C. F. McDonald, and C. P. Howard, Book No. G00183, HTD-Vol. 10, ASME, New York, 1980, pp. 57-64.
- 13 Cassie, A. B. D., "Adsorption of Water Vapor by Wool Fibers. Part II—Theory of Propagation of Temperature Change," *Transactions of the Faraday Society*, Vol. 36, 1940, pp. 453-465.
- 14 Lighthill, M. J., and Whitham, G. B., "On Kinematic Waves," *Proceedings of the Royal Society of London*, Vol. A229, 1955, pp. 281-345.
- 15 Coppage, J. E. and London, A. L., "The Periodic-Flow Regenerator—A Summary of Design Theory," *ASME Transactions*, Vol. 75, July 1953, pp. 779-787.
- 16 Dunkle, R. V., Banks, P. J., and Ellul, W. M. J., "Regenerator Research, Development, and Applications in Australia—1978 Status," *International Journal of Refrigeration*, Vol. 1, No. 3, Sept. 1978, pp. 143-150.
- 17 Dunkle, R. V. and Maclaine-cross, I. L., "Theory and Design of Rotary Heat Exchangers for Air Conditioning," *Mechanical and Chemical Engineering, Transactions of The Institution of Engineers, Australia*, Vol. MC6, No. 1, May 1970, pp. 1-6.
- 18 Dunkle, R. V., Banks, P. J., and Maclaine-cross, I. L., "Wound Parallel Plate Exchangers for Air-Conditioning Applications," *Compact Heat Exchangers—History, Technological Advancement and Mechanical Design Problems*, edited by R. K. Shah, C. F. McDonald, and C. P. Howard, Book No. G00183, HTD-Vol. 10, ASME, New York, 1980, pp. 65-71.

APPENDIX

The basic experimental apparatus used for this investigation is described in [16]. Four modifications were made to this apparatus to allow testing for the desired results: a new regenerator was constructed, a fast-response split-duct heater was designed and constructed, the temperature measuring devices were replaced, and the duct configuration was modified.

The regenerator was constructed by spirally winding a polyester film around an aluminum hub [17, 18]. The spirals are separated by aluminum spacers held in spokes to produce parallel flow passages. The polyester film is 0.125 mm thick and the flow passages are 0.914 mm wide giving a matrix porosity to air flow of 88 percent. The regenerator has a length of 160 mm and an effective cross-sectional area of

0.0935 m² per period. The properties of the matrix are such that the conductivity assumptions of the theoretical model are justified. The polyester film is thin enough that axial conduction effects are negligible and the resistance to heat transfer into the film at any position is small compared to the matrix-fluid convective transfer resistance. Airflow through the matrix was at a Reynolds number of the order of 100, so that the convective transfer coefficient for the numerical model was predicted assuming laminar flow [3, 17].

A fast-response, split-duct heater was designed to balance the trade-offs between rapid heater response, low heater wire temperature, and high power output. The heater has a response time of approximately 5 s and a power output of up to 3.6 kW. It is constructed to provide spatial nonuniformities as in Fig. 4 with $\beta_s = 0.5\beta_1$.

Thermocouple grids are located immediately upstream and downstream of the regenerator in each flow stream, which allows measurement of both spatial average temperatures and temperature distributions. The error in temperature measurement including radiation effects, is estimated to be 2 percent of the total temperature difference across the regenerator.

The ductwork was modified to allow testing of a regenerator operating under unbalanced flow conditions. The flow rates of the two fluid streams are controlled by separate fans. Flow nozzles are located in each fluid stream, measuring flow rates to within an estimated error tolerance of 1.8 percent. At the regenerator, the two fluid streams are separated by clearance seals, with an average clearance of 1.1 mm. Corrections for the effects of fluid stream mixing due to leakage are made as in [17].

Preliminary tests indicated that the velocity was uniform to within ± 10 percent with the regenerator removed. Since the matrix forms the largest flow resistance in each stream, the uniformity of the distributions was expected to improve with the regenerator in place. The temperature distribution with the matrix in position was uniform to within ± 3 percent, implying similar uniformity of velocity. Analyses of the regenerator operating under steady periodic conditions showed conservation of energy to within 5 percent.

